Annals of Clinical and Medical Case Reports

Pioneering Research ISSN 2639-8109 | Volume 12

The Invention of the Mid-Infrared Generating Atomizer and its Human and Veterinary Medicinal Applications– A Pioneering Research

Umakanthan T[1]*, Madhu Mathi[2], Umadevi U[3]

[1]Veterinary hospital, Gokulam Annadhanam Temple Complex, Plot no.: 1684, Meenavilakku-Meenakshipuram Road, Anaikaraipatty Post, Bodinayakanur Taluk, Theni Dt, Tamil Nadu, India – 625582

[2]Veterinary hospital, Vadakupudhu Palayam, Erode Dt, Tamil Nadu, India – 638152.

[3]Assistant Professor, Department of Botany, The Standard Fireworks Rajaratnam College for Women, Sivakasi, Virudhunagar (Dt), Tamil Nadu, India – 626 123

***Corresponding author:**

Umakanthan T,
Veterinary hospital, Gokulam Annadhanam Temple Complex, Plot no.: 1684, Meenavilakku-Meenakshipuram Road, Anaikaraipatty Post, Bodinayakanur Taluk, Theni Dt, Tamil Nadu, India

Received: 02 Jan 2024
Accepted: 25 Jan 2024
Published: 29 Jan 2024
J Short Name: ACMCR

Citation:

Umakanthan T, The Invention of the Mid-Infrared Generating Atomizer and its Human and Veterinary Medicinal Applications– A Pioneering Research. Ann Clin Med Case Rep. 2024; V12(13): 1-25

Keywords:

MIRGA; 2-6 µm mid-infrared; Human; Veterinary; Diseases; Therapy; Cure; Easy; Economical

1. Abstract

1.1. Background and Objectives: In the current scenario, there are different therapies for different diseases of human and animals. The existed therapies are associated with hurdles like drug resistance, less sensitivity, side effects, uneconomical, etc. However, none of the therapies provide multi-disease management on a molecular basis. Every disease originates due to inter and/or intra-molecular (cell/ tissue) changes, which changes their respective chemical bonds. Therapies focusing to rectify the molecular changes (molecular medicine) are growing slowly, which could act as a single remedy, but needs extensive multi-faculty research.

1.2. Method: By studying and comparing the basis of modern and traditional therapy, we have developed a 2-6 µm mid-infrared generating atomizer (MIRGA).

1.3. Result: The hand-held MIRGA contains live ions in aqueous medium. During spraying, the emitted ions oscillate, generate 2-6 µm mid-infrared energy, which penetrates the intervening media and acts on the lesions, hence cure occurs.

1.4. Interpretation and conclusion: We analyzed for MIRGA therapeutic effect against various wounds and co-morbidities including malignancy in human and animal patients. On providing treatment for various periods of times, we observed significant improvement in the disease condition which provide evidence regarding potential of MIRGA in the medical and veterinary fields. MIRGA is safe, affordable and easy-to-use.

2. Introduction

All the animate (including any living body) and inanimate matters on the Earth are composed of atoms (Ganesan, 2003) which are held together by chemical bonds (Alberts et al., 2002). The continuous vibration of the living body molecules generates electromagnetic radiation (10 µm) (Verheest, 2000; Sanders, 2014) in the range of infrared (DeVries, 1994; Dakin et al., 2018). In addition, 66% of Sun's radiant energy that we receive daily on Earth is infrared (Aboud et al., 2019), which is a known therapeutic agent for the treatment of some medical conditions (Rojas et al., 2011; Barolet et al., 2015), and it is also applied in veterinary practice (Chen et al., 2015; Perego et al., 2016; Nagaya et al., 2018) and aesthetical purposes (Wardlaw et al., 2019). Mid-infrared (mid-IR) is the portion of infrared radiation whose wavelengths are comprised between 2-10 µm (Grassani et al., 2019). Living cells contain a huge number of molecules (water, carbohydrates, proteins, lipids, nucleic acids…) that are active in the mid-IR region, since

the vibrational frequencies of their chemical bonds are located in this radiation range. (Toor et al., 2018). Photostimulation and photomodulation is possible in living cells because they are mainly composed by water (Musumeci et al., 2014; Pollack, 2015) and changes in the nanostructured water layers can be triggered upon application of mid-IR radiation, since water molecules absorb in this region. (Sommer et al., 2008; Sommer et al., 2011). The absorption of mid-IR radiation by water molecules causes transitions between vibrational and changes in the vibrational modes (twisting, stretching, bending) (Mohan, 2004; Agarwal et al., 2014; Tsai et al., 2017), and it could lead to the rupture of some weak chemical bonds (Flynn et al., 1996) leading to the formation of new molecules (Datta et al., 2014; Xu et al., 2017). These physicochemical alterations can affect different processes, such as cell repairing, inflammation reduction, and pain relief (Nouri, 2018) occur. For these reasons, mid-IR has potential applications in the biomedical field. At present, the invented and marketed mid-IR emitters are uneconomical and mostly confined to military, biomedical research and diagnostics (Toor et al., 2018).On one hand, the invention of MIRGA entails the development of an affordable, safe, and convenient mid-IR emitter.

On the other hand, many traditional healing therapies, such as healing touch, magnet therapy, acupuncture, polarity therapy, reiki, aura balancing, and johrei, are based on methods (photobiomodulation, photostimulation) in which healers used infrared radiation from their hands (Schoonover, 2003; Oschman, 2016) to interact with the patient's electromagnetic fields and ultimately, try to achieve pain relief or improvement of the patient's condition. Hence, electromagnetism is in the basis of many phenomena involving atomic and molecular entities (Dugdale, 1993).

Like this, we analysed, compared and combined multi-faculty modern and traditional facts and findings. It is well known that cells are composed of atoms thereby molecules, and these entities are able to interact with electromagnetic radiation (they can absorb and emit certain radiation wavelengths). Keeping this in mind, we hypothesized that the alteration of the interaction between cells and electromagnetic radiation could cause physiological effects that could lead to the development of mild to severe pathologies (diseases that exhibits symptoms). Also application of electromagnetic radiation externally could be used to relieve such symptoms and to ultimately improve the patient's health condition. We designed MIRGA as a hand-held 2-6 μm mid-IR emitter that can be used by physicians or patients themselves for therapeutic purposes. Herein, we explained the successful clinical outcomes of MIRGA in patients with wounds of diverse aetiology. Additionally, we performed a retrospective study on the concurrent diseases both in human and animal patients. Using different instrumentations, we also tried to identify the MIRGA's effect at a cell and an atomic level.

3. Material

3.1. MIRGA

MIRGA (patent no.: 401387) is a 20 ml pocket sized atomizer containing inorganic water based solution in which approximately two sextillion cations and three sextillion anions are contained. During spraying, depending on pressure (vary with the user) applied to plunger, every spraying generates 2-6μm mid-IR. Design of the MIRGA and emission of 2-6μm mid-IR has been presented in detail by Umakanthan et al., 2022a; Umakanthan et al., 2022b; Umakanthan et al., 2023c; Umakanthan et al., 2023d. Every time spraying emits 0.06ml which contains approximately seven quintillion cations and eleven quintillion anions. (details about MIRGA available in supplementary content C1)

The chemical compounds used in MIRGA spraying are a perspective for biomedical applications (Tishkevich et al., 2019; Dukenbayev et al., 2019). It is also a new synthesis method for preparation of functional material (2-6 μm mid-IR) (Kozlovskiy et al., 2021; El-Shater et al., 2022). It is well known that the combination of different compounds, which have excellent electronic properties, leads to new composite materials, which have earned great technological interest in recent years (Kozlovskiy and Zdorovets, 2021; Almessiere et al., 2022).

3.2. Cellular Morphology Analysed Using Instruments

i)"K87" Human dermal fibroblast. Images were acquired Phase contrast microscopy (Zeiss AxioVert 200 M microscope using AxioVision 4.8 software (Carl Zeiss, Germany))

ii)HPV16 Cervical cancer cell line "SiHa". Fluorescent test with DAPI staining done. Dye used: DAPI (4′,6-diamidino-2-phenylindole). Confocal laser scanning microscope (LSM 510 META, Carl Zeiss Inc., Thornwood, NY) equipped with an argon laser using FITC filter.

iii)FTIR of Dog's aorta (DNA, Protein and Lipid isolates) and kidney (Protein isolate) (autopsy specimen). FTIR instrument used was of Model -3000 Hyperion Microscope with Vertex 80 FTIR System, make - Bruker, Germany.

iv)3D fluorescence spectroscopy of dog liver (DNA isolate) (autopsy specimen) using JY Fluorolog-3-11 spectroflurometer.

3.3. Clinical Trials

The present study was approved by the Institutional Ethics Committee (certificates available in Supplementary Figure 1, Figure 2) and all methods were performed under the strict guidelines and regulations. The studied patients had acute and chronic skin wounds and/ or haemorrhoids of various degrees and aetiologies (Table 1). MIRGA spraying was done from 0.25-0.5 meter towards the lesions. Retrospective study involved: nearly 800 human patients who were primarily treated for wounds with MIRGA, also evidenced simultaneous relief from their co-morbidities (Table 2).

MIRGA therapy recovered patients under the supervision of veterinarians had also treated their domestic animals. Those 60 animals were with diverse diseases, from mastitis, wounds, inflammation, skin diseases including allergy and epithelial benign and malignant cancer (Table 3). Those animals did not receive any treatment or medication except MIRGA spraying.

4. Method

On a general rule, MIRGA has to be sprayed externally over the lesion (irrespective of visceral or epidermal) from a distance of 0.25 to 0.50 meter (method of spraying video link available in Supplementary video V1). The generated mid-IR can penetrate the intervening media by patients' clothing material made up of cotton, polyester, wool, synthetic fibre, and others. Thus MIRGA can be sprayed 0.25 to 0.50 meter above the site of lesion (eg. visceral cancer) without (or) removing the clothing. Direct spraying without clothing material is also equally effective. This distance is essential for the MIRGA's sprayed solution to be able to form ion clouds which oscillate, mid-IR radiation is generated, and scatter. Thus scattered non-ionizing mid-IR radiation is absorbed by the affected cells, interact with their molecules, causing variations in their vibrational states and result in an improvement from pathological condition.

4.1. Cell Line Studies

Three types of laboratory studies performed.

i)Effects of MIRGA spraying on "K87" Human dermal fibroblast

The cells from cell line were seeded on two culture plates. Two MIRGA sprays were applied to one plate, and no spray was applied to the other one (control). After four days, images were acquired.

ii)Effects of MIRGA spraying on HPV16 Cervical cancer cell line "SiHa"

Cells from the cell line were grown in two culture plates. One of the plates was sprayed twice with MIRGA, and the other one which was not sprayed, served as control. Fluorescent test with DAPI staining done following the protocol of DAPI Protocol for Fluorescence Imaging by ThermoFisher Scientific, and the cells were observed.

iii)Effect of MIRGA spraying on SARS-CoV-2 virus

4.2. Animal Studies - Effects of MIRGA Spraying on Dog Aorta, Kidney and Liver Samples

Being terrestrial mammals, the anatomy and physiology of dogs and humans are closely related. Hence, we selected dog aorta samples to study the effect of MIRGA at cellular level in a tissue. Aorta is the largest artery of dog and human body, and its tissue is unique for its thickness, histological complexity, great elasticity and distensibility. All these features have biomechanical implications related to the Windkessel effect. For this study, four pieces of the same size from dog aorta (autopsy specimen) were cut and each one was packed in 70 µm thick polythene pouch that was sealed with cellophane tape and labelled as C, 1S, 2S, and 3S. Correspondingly, 0, 1, 2, and 3 MIRGA sprayings were applied externally over the polythene pouch. After MIRGA spraying, DNA, lipid and protein fractions were isolated from these samples. In addition, dog's aorta kidney and liver samples were harvested from the autopsied carcass and the procedure applied to the aorta samples was followed. To kidney samples, 0, 1 and 3 MIRGA sprays were applied. Then the protein fraction of the samples isolated. These isolates were individually subjected to FTIR to study potential changes at molecular level. To liver samples, 0, 1 and 2 MIRGA sprayings were applied, DNA isolated, and subjected to 3D fluorescence spectroscopy.

4.3. Human Clinical Trials

The patients were administered one or two or in some cases more MIRGA spraying twice daily until complete recovery was achieved and the analysis was done by comparing pre and post MIRGA treatment medical reports (Table 1). During the treatment, the patient was not administered any additional medication. The patients were closely monitored for the healing of the condition/adverse events. Control patients were treated with usual antibiotics and dressing.

4.4. Animal Clinical Trials

The spraying technique and studies were similar to human and animal patients. Retrospective studied human and animal patients were with or without routine medical therapy.

5. Results and Discussion

5.1. Effects of MIRGA Spraying on Human Dermal Fibroblasts

The cells in the control and MIRGA treated group were similar, spindle-like, in shape. However, change in confluency, 100% in control, and 70% in sprayed cells, was observed after 4 days of spraying. The change in confluency was most likely due to cell cycle arrest caused by the MIRGA spraying. We also observed slightly bigger and flat cells, which was most likely due to the spray treatment. The major difference between the control and the MIRGA sprayed sample is the difference in confluency, which is due to cell cycle arrest caused by the spray treatment. The images did not display any differences in cell death. (Figure 1)

5.2. Effects of MIRGA Spraying on Cells from a Human Cancer Cell Line

Mid-IR radiation produced nuclear changes (Figure 2). On analyzing the nuclei we observed nuclei damage due to MIRGA treatment. The nuclei in the control group were oval with a clearly defined nuclear border, and no prominent nucleoli or mitoses were observed. However, the nuclei in the MIRGA sprayed treated group showed marked anisokaryosis and different shapes from oval to polygonal with mostly hypochromatic fine granular chromatin. The spray treatment also increased the number of polynucleated cells (marked in red circles), which indicates complications during

the mitotic process leading to a decrease in cell growth and cell cycle arrest.

5.3. Effect of MIRGA Spraying on SARS-CoV-2 Virus

In vitro antiviral assay studies using Vero cells infected with SARS-CoV-2 revealed 95% quantitative virus reduction. (certificate available in Supplementary Figure 3)

5.4. FTIR Experiments on DNA, Lipid, and Protein Isolates from Dog Aorta Samples

(Supplementary Figure 4) (Raw data in Supplementary data D1 and detailed interpretation in Supplementary content C2)

5.4.1. DNA Fraction

Control: Absorption peaks at 3778 cm-1 (OH), 2920 cm-1 (CH), 1623 cm-1 (C=C), 1470 and 1408 cm-1 (CH), and 1042 cm-1 (CO-O-CO) were observed. It has strong peak at 3440 cm-1 showing the OH group (stretch H bonded, strong broad) along with the above mentioned peaks.

1 sprayed Sample: Absorption peaks at 3778 cm-1 (OH), 2922 cm-1 (CH), 1644 cm-1 (C=C), 1471 and 1411 cm-1 (CH), and 1044 cm-1 (CO-O-CO) were observed. It has strong peak at 3440 cm-1 showing the OH group (stretch H bonded, strong broad) along with the above mentioned peaks. Extra peaks (compared to the control sample) are observed at 1251 (due to CO), and 500-600 cm-1 (due to the C-X groups).

3 Sprayed Sample: Absorption peaks at 2888 cm-1 (CH), 1634 cm-1 (C=C), 1469 and 1410 cm-1 (CH), and 1044 cm-1 (CO-O-CO) were observed. It has strong peak at 3441 cm-1 showing the OH group (stretch H bonded, strong broad) along with the above mentioned peaks. Extra peaks (compared to the control sample) are observed 500- 600 cm-1 (due to the C-X groups). The peak at 3778 cm-1 observed in the previous 2 samples more or less disappeared.

To conclude, Peaks at 2888-2922 cm−1 assigned to the C-H stretching (Mohan, 2004) of an aliphatic group indicates the existence of methyl and isopropyl substituents. The peak due to the C=C has shifted from 1623 cm-1 in the control sample, to 1644 and 1634 cm-1 in the samples sprayed once and three times, respectively, suggesting a chemical interaction (Xu et al., 2017). There are extra peaks in the sprayed samples due to C-X groups which also suggest a change in the structure of the DNA (from C=C to C-X)due to the MIRGA spraying. Also, the lack of peak at 3778cm-1 in the three times sprayed sample (which is present in the control sample and the sample sprayed once) suggests further changes caused by more sprayings.

5.4.2. Protein Fraction

Control: Absorption peaks at 2922cm-1 (CH), 1635 cm-1 (C=C), 1511, 1462 cm-1 (CH), 1218 cm-1were observed. It has strong peak at about 3397 cm-1 showing the OH group (stretch H bonded, strong broad) along with the above-mentioned peaks. A peak is observed at about 3886 cm-1(due to C-O bonds in C-OH groups) and strong and broad peak is observed at 592 cm-1 (CH groups). Peak at 947 cm-1is due to the C-C.

1 Sprayed Sample: Absorption peaks at 2925 cm-1 (CH), 1636 cm-1 (C=C), 1541, 1464 and 1364 cm-1 (CH), 1218cm-1were observed. It has strong peak at 3448 cm-1 showing the OH group (stretch H bonded, strong broad) along with the above-mentioned peaks. The peaks observed at about 3886 and 592 cm-1 in the Control sample are much weaker in 1 sprayed sample. Peak at 949cm-1is due to the C-C has more intensity than the control.

3 Sprayed Sample: Absorption peaks at 2923cm-1 (CH), 1636 cm-1(C=C), 1544, 1460 and 1364 cm-1 (CH), 1218cm-1were observed. A new peak at 1111 cm-1is observed due to C–O stretch. It has strong peak at 3447 cm-1 showing the OH group (stretch H bonded, strong broad) along with the above-mentioned peaks. The peaks observed at about 3886 and 592 cm-1 in the Control sample are more or less disappeared in 3 sprayed sample. Peak at 940cm-1is due to the C-C has much more intensity than the control.

To summarize, Peaks at 2881-2955 cm−1 assigned to the C-H stretching of an aliphatic group indicates the existence of methyl and isopropyl substituents. The peak at 1111 cm-1 (C-O) and increased intensity of the C-C peaks in the three-times sprayed sample suggests a change in the protein structure by the increasing temperature (Kowacz et al., 2017) upon more spraying (denaturation).

5.4.3. Lipid Fraction

Control: Absorption peaks at 2922, 2956, 2852 cm-1 (CH), 17431627 cm-1 (C=C), 1548, 1462 and 1380cm-1 (CH)were observed. It has strong peak at 3440 cm-1showing the OH group (stretch H bonded, strong broad) along with the above-mentioned peaks. Some weak peaks at 600-800 cm-1are observed due to the C-X bands.

1 Sprayed Sample: Absorption peaks at 2923, 2956, 2851 cm-1 (CH), 17371622 cm-1 (C=C), 1544, 1462 and 1377 cm-1 (CH) were observed. It has strong peak at 3443 cm-1 showing the OH group (stretch H bonded, strong broad) along with the above-mentioned peaks. A clear peak at 1215 cm-1is observed which is normally indicates changing the lipid conformation to Z form. A new peak at 1020 cm-1is observed due to CO-O-CO (change in the Lipid inter structure). The peaks at 600-800 cm-1are increased due to the raise in the number of C-X bands upon one spraying.

3 Sprayed Sample: Absorption peaks at 2923, 2956, 2852 cm-1 (CH), 17401623 cm-1(C=C), 1547, 1464 and 1380 cm-1 (CH) 1082 were observed. It has strong peak at 3442 cm-1 showing the OH group (stretch H bonded, strong broad) along with the above-mentioned peaks. Similar to DA1, a clear peak at 1215 cm-1is observed which normally indicates changing the Lipid conformation to Z form. The peak observed at 1020 cm-1in the DA1 sample disappears in the 3 sprayed sample suggesting breakage

of the structure from CO-O-CO band. The number of the peaks at 600-800 cm-1are also significantly increased due to increasing the number of C-X bands upon three spraying.

To conclude, Peaks at 2881-2955 cm−1 assigned to the C-H stretching of an aliphatic group indicates the existence of methyl and isopropyl substituents. The peak at 1215cm-1 that appears upon MIRGA spraying suggests changes in the lipid conformation to Z form. The peak at 1020 cm-1 in the one sprayed sample suggests the formation of CO-O-CO groups. However, this peak disappeared upon three spraying showing breakage (McMakin, 2011; Moss, 2011) of this band. More peaks at 600-800 cm-1 (C-X groups) in the three-times sprayed sample also reconfirms this.

5.4.4. FTIR on Dog kidney Sample – Protein Isolate (Supplementary Figure 5)

Control: shows a broad band between 3600-3200 cm-1 which is attributable to N-H stretching of amine and amide groups. A more defined, multiple bands appears between 2800-3000 cm-1, which are typical of the C-H stretching of saturated moieties, like alkanes. Very intense peaks are observed around 1640 cm-1 and 1040 cm-1, attributable to the stretching of C=O and C-O bonds, respectively. Below 1500 cm-1 the fingerprint region is located. This region is usually very crowded and it is difficult to identify peaks accurately (Figure 4).

3 Sprayed Sample: shows a spectrum with a significantly higher transmittance (less absorption), pointing to a reduced concentration of the compounds giving rise to the observed bands. Bands and peaks observed in this sample are quite similar in shape and position compared to the control sample.

1 Sprayed Sample: shows a spectrum with a higher transmittance compared with 3 sprayed sample, and remarkably higher than the transmittance of the control sample. This indicates that a reduction in the concentration of the compounds (Yi, 2012; Esmaeili, 2015) originating the bands and peaks occurs in 1 sprayed sample compared to the 3 sprayed sample and, especially, compared to control sample. Bands and peaks observed in this sample are quite similar in shape and position compared to the control and 3 sprayed samples, except for the fact that the N-H and C-H stretching bands are missing.

To conclude, one-time MIRGA spraying caused the almost complete loss of the signals coming from O-H and N-H stretching, and from C-H stretching, whereas the C=O and C-O stretching bands are strongly reduced. This is related to a drastic reduction in the concentration of the biomolecules (Esmaeili, 2015) present in the sample. Explanation for this observation is that the effect of mid-IR on the aqueous sample could cause a temperature increase enough to favor protein precipitation (denaturation) (Kowacz et al., 2017). The effect of mid-IR on the sample could break the interactions that keep the proteins well-folded and in solution. In this context, many partially or unfolded proteins could establish intermolecular interactions leading to a precipitate.

On the other hand, spraying three times resulted in an augmentation of the absorbance of the sample, pointing to a higher concentration compared to the sample which was sprayed once. However, the increase in the absorbance level was below the control. The repetition of excess MIRGA spraying rises temperature enough to solve again the part of the precipitated protein. The intermolecular interactions between unfolded proteins could be broken, and part of the proteins would be able to refold and recover totally or partially their native structures, being again soluble. Based on the fact that mid-IR radiation is able to induce changes in the water layers surrounding biomolecules (hydration shell), such as proteins, these changes are known to promote attractive interactions among biomolecules, which can trigger their clustering and precipitation. This could be the reason of a drastic decrease of protein concentration and diminution or disappearing of IR signals in the spectrum. (Kowacz et al., 2017; Kowacz et al., 2018)

With the FTIR result, it can be inferred that the MIRGA spraying at recommended optimal dose i.e. spraying once, has significantly reduced the excess protein deposition from kidney (renal diseases) which might promote recovery; whilst excessive MIRGA spraying i.e. spraying three times, have started to reverse the effect of one-time spraying.

5.4.5. 3D Fluorescence Spectroscopy on Dog Liver sample – DNA Isolate

(Supplementary Figure 6) (Raw data in Supplementary data D2)

The 3 fluorescence fingerprints are characterized by an island contour. The control sample has contour centered at (Ex = 283 nm, Em = 362 nm). The mid-infrared irradiated sample has a contour centered at (Ex = 300 nm, Em = 402 nm). The emission is centered primarily on the 360 nm - 400 nm region of the visible spectrum. A weak fluorescence in the 520 nm region of emission can be seen when the excitation is in ~ 260 nm. This emission can be the tail end of the green emission observed in the works of Volkov et al., 2018. There is a significant shift in the fluorescence peak when the sample has been irradiated by mid-infrared. In terms of fluorescence emission theory, the shift to lower emission wavelength is a result of lowered transition energy from the excited state to ground state. It appears that the exposure to mid-IR rays results to altered energy diagram of the DNA from the dog liver. (Figure 5).

In principle, mid-IR energy is generally absorbed by chemical bonds within molecules/ atoms leading to increased vibrational modes such as twisting, stretching, and bending. Both kinds of energy may transform and dissipate into other molecular vibrations in the form of increased thermal energy (Tsai et al, 2017). The increased exposure to the mid-infrared has caused the island contour to increase in broadness and the fluorescence intensity, i.e. the prolonged exposure to the IR rays increased the quantum yield of the DNA sample.

Thus, the action of MIRGA at subatomic level is also relatively better demonstrated (than stoichiometric/ fluorescence staining) to be responsible for its clinical efficacy.

5.4.6. Human Clinical Results

During the clinical trial with MIRGA, a few patients reported an improvement of other co-morbidities that they were suffering from. The first case was a patient with psoriasis and cervical spinal cord compression. MIRGA spraying was applied to alleviate psoriasis, but simultaneously the patient reported relief from the cervical pain. From the patient's feedback, it is recorded that within 1-2 minutes of MIRGA spraying, the patient was able to rotate the neck all around. After feeling this comfort, the patient checked and verified the same relief every time upon MIRGA spraying. This has led us to take up a retrospective analysis of MIRGA's action on other patients with coexisting ailments, which were confirmed by radiographic and histopathological diagnosis. These patients used one, two, or more MIRGA sprayings. The detailed findings were presented in (Table 2).

*The cancer patients were MIRGA sprayed 0.25–0.50 meter from skin irrespective of cutaneous/ visceral malignancy.

Note: Please check this link for video/ audio testimonials for the cases enlisted in (Table 2). https://drive.google.com/open?id=1_1h-WN56JIZkjeNmSG9YLag_wsCkmz2ba

The course of time for cure by MIRGA is 40-60% less when compared to other therapeutic systems.

Based on the experience and recommendations of our successfully trialled patients' advice and guidance, hundreds (nearly 800, as far as we know) of various diseased (single/multiple) patients used MIRGA by themselves or under doctor's supervision and got recovered. These patients' diseases included a variety of benign tumors and malignant cancers (including leukemia), chronic aphonia, deafness, etc. Some patients declared to have used only MIRGA without any additional specific medicine. On contrary, some patients who reported recovery signs of their coexisting diseases after MIRGA therapy has stopped/ reduced their routine therapy.

In early malignant patients, MIRGA spraying clinically recovered them. On contrary, in some chronic patients MIRGA sprayings gradually improved their health condition to a peak level, then remained static and further MIRGA spraying was ineffective. These patients on integrated therapy with MIRGA showed remarkable recovery. Interestingly in all animal malignancy MIRGA spraying alone observed to be very effective.

5.5. Veterinary Clinical Results

We, the two authors, being veterinarians, our experience in veterinary therapy (one with 40 years in clinics) has taught that, treating malignancy with allopathic medicine involves more expense, side effects, longer course of therapy and lesser percentage of recovery. We experienced that MIRGA could be an alternate choice to treat variety of diseases with ease in relatively short time and economical. In human and veterinary retrospective MIRGA study, the cancer mass after spraying either completely or partly disappear or retained the original dimensions but the patient's showed recovery. There was no evidence of MIRGA's side effects and recurrence. It was found that the wounds and diseases healed faster than usual and without any secondary complication.

6. Definition of MIRGA

Umakanthan et al., 2022a and Umakanthan et al., 2023d has discussed about the invention background, technique of mid-IR generation and safety assessment of MIRGA through toxicological study. Thus, MIRGA is defined as 'a harmless, economical atomizer containing an imbalanced ratio of ions suspended in water, which influence the natural potency of target substances by generating mid-IR while spraying'. (detailed discussion on MIRGA available in Supplementary content C3)

7. Action of MIRGA Emitted 2-6 µm mid IR on the Target Substances

While spraying MIRGA, most of the mid-IR energy scatters through the air and gets absorbed by receptors molecules, i.e. diseased cells. Virtually all organic molecules (pathological cells) absorb mid-IR radiation which causes a change in the molecule's vibrational state to move from the lower ground state to excited higher energy state (Girard, 2014). This leads to changes in pathological cells' chemical bonds (Mohan, 2004; Shankar, 2017) which in turn caused consequent changes in the molecule's physical and chemical characteristics, configuration and compound transformation depending on the dose of energy applied (Atkins et al., 2011; Yi, 2012; Datta et al., 2014; Esmaeili, 2015), thereby changes in the cell pathology which effects cure.

The action of mid-IR radiation on cells involved in pathological conditions, especially in cancer, was already discussed by different authors. (Lee et al., 2005; Chang et al., 2013; Chang et al., 2015; Tsai et al., 2017)

There are two major disadvantages of conventional medical therapy; specific treatment for every single disease, and the presence of multiple diseases results in the compromise of the treatment (Scanlan, 2011). Besides, sometimes the multiple disease treatment is expensive and complex. Diseases occur due to molecular changes during the cell cycle, which is viciously neglected by the disease management system. (Dossey, 1992; Fenton et al., 1998). MIRGA has overcome both the limitations by exerting action at molecular level as proven in our instrumentation results, and successfully cured the coexisting diseases. It is also observed from the cases summarised in (Table 2) that MIRGA has not disrupted or interfered with any of the allopathic treatments or other medical therapies. Hence, MIRGA can be used as a single therapy or as an adjunct to an allopathic medicine system. Manufacturing cost of one MIRGA unit giving 300 spraying is approx. 0.35 USD. It is

portable and easy to use by patients/ medics/ vets than the present marketed mid-IR emitters.

8. Past Interests

Our in vitro and clinical studies showed that the MIRGA's chemical formulation, therapeutic effect, and outcomes were significantly similar to that of 'The Superior Medicine' of various ancient medicinal systems such as 'Muppu' (Tamil Siddha), 'Al-Kimiya' (Arabic), 'Rasayana' (Indian Ayurveda), 'Rasavatan' (Persian), Materia prima, Philosopher's stone, Tincture (Europe) and Taoist alchemy, Hudan, or Jindan (Chinese). Also, hand healing therapy using body-generated infrared is similar to MIRGA spraying. Moreover, we witnessed, the sages and saints (now living in remote parts of the Indian mountains) used to sprinkle holy water on the patients to cure diseases. This involves the mid-IR radiation generated by their palms, water velocity and body which is transferred to the patients.

9. Future Interests and Conclusion

The invented MIRGA has demonstrated its portability, safety, and cost-effective use in therapeutic purposes. The generated mid-IR radiation exerted alterations at a molecular/ atomic level in the affected cells and promoted faster recovery from diseases. We have also witnessed that the mid-IR radiation's effectiveness to cure the coexisting diseases, in relatively shorter treatment duration than other medical systems. With MIRGA's potential action and observed effect, further investigations of its efficacy in other diseases are ongoing. The in vitro studies showed MIRGA-induced changes in the cell morphology. However, this should be studied in-depth to understand the mechanism of action of MIRGA and its possible role in the treatment of various cancers and other potential fields. Also, with our nearly two-decade experience with MIRGA, we assume that, by altering MIRGA's chemical formulation and atomizer dimension; through future research it is possible to obtain better results than now.

10. Data and Materials Availability

All data is available in the manuscript and supplementary materials.

Supplementary file available in:

https://docs.google.com/document/d/1p3WXKN9xnEEfjrgfpNoj5OWmKs1DxcRk/edit

11. Funding

The authors received no specific funding for this research.

12. Author Contributions

Umakanthan: Conceptualization, Methodology, Resources, Supervision, Validation.

Madhu Mathi: Investigation, Visualization, Writing - Original draft preparation.

Umadevi: Data curation, Project administration.

Umakanthan, Madhu Mathi: Writing- Reviewing and Editing.

13. Competing Interest

In accordance with the journal's policy and our ethical obligation as researchers, we submit that the authors Dr.Umakanthan and Dr.Madhu Mathi are the inventors and patentee of Indian patent for MIRGA (under-patent no.: 401387) which is a major material employed in this study.

14. Acknowledgement

Authors thank multi-Faculty scientists of different labs, institutions, universities, etc., around the world for their technical guidance and help; also thank Dr.George Tranter, Chiralabs Ltd., Begbroke Centre for Innovation & Enterprise, Oxfordshire, UK; Dr. Jan IC Vermaak, Manager of Engineering, Nuclear Science Center - Texas A&M University, USA; Dr.TakashiroAkitsu, Professor, Department of Chemistry, Faculty of Science, Tokyo University of Science, Japan; Dr.Kam-Hung Low, X-ray Facility manager, Department of Chemistry, The University of Hong Kong; Ms. SatitaphornSriphuttha, Tokyo University of Science, Japan; Ms.Shiho Murakami, Mr.Kanai and other Spectroscope specialists of Hitachi High-Tech, Japan; Mr. Gary Powell, Lightwind corporation, Petaluma, California, USA; Dr.Senthil Kumar Rajendran, Cell Biology, Biosciences, ÅboAkademiUnivesity, Finland; Dr. Ramakrishnan, Head, Indian Veterinary Research Institute, Mukteshwar, India; Dr. R Prabhakaran, Assistant Professor, Department of Chemistry, Bharathiar University, Coimbatore, India; Dr.Adriana Pietrodangelo, PhD, C.N.R. Institute for Atmospheric Pollution Research, Italy; Dr. Héctor Zamora Carreras, Post-doctoral assistant, Rocasolano Institute of Physical Chemistry, Spain; and other Kolabtree experts; All financiers who funded this research for nearly 2 decades; And we would also like to apologize to all scientists and other helpers around the world who are not cited here now.

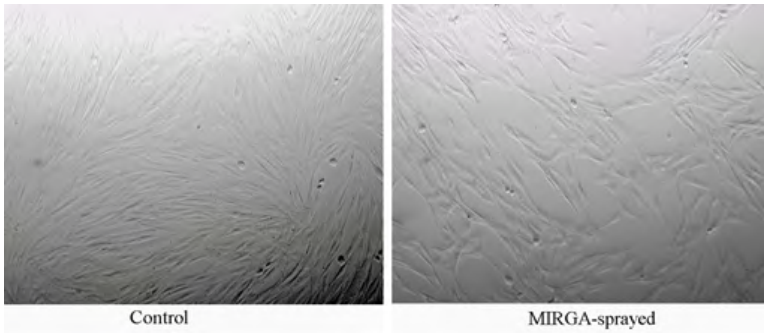

Figure 1: MIRGA's effect on human dermal fibroblasts

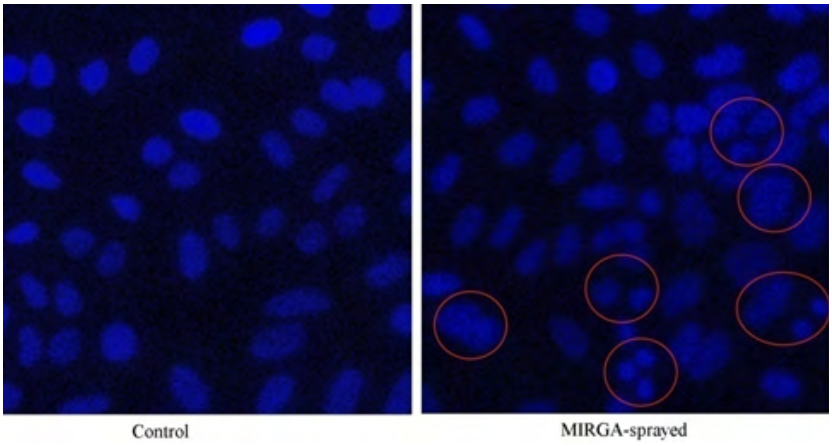

Figure 2: MIRGA's effect on cancer cells observed with the fluorescence test

Figure 3: Third-degree burn wound treatment using MIRGA spray

Figure 4: Treatment of severe psoriasis in back using MIRGA spray

Figure 5: Treatment of vitiligo in an adult and child using MIRGA spray

Figure 6: Treatment of chronic eczema in leg using MIRGA spray

Figure 7: Treatment of squamous cell carcinoma in vulval lip of a cow using MIRGA spray

Table 1: Types of human medical conditions and treatment course by MIRGA spraying (respective images available in Supplementary Table T1)

No.	Disease	Course for the complete cure with MIRGA spraying	Normal time for the complete cure using other medicines as in literature
1	Severe ulcer in thumb toe	15 days	12 to 20 weeks
2	Chronic varicose ulcer in dorsal and lateral sides of the foot	Granulation started on 27th day	3 – 4 months (Collins et al., 2018)
3	Diabetic wound in sole of the foot	15-25 days	Healing takes weeks or months, and one-third of ulcers never heal with amputation as the consequence.
4	Third-degree burn wound (Fig 3)	Burn healed and skin regeneration started by 14th day	Often take greater than 3 weeks to heal or need skin grafting (American Family Physician, 2000)
5	Psoriasis in hand	Itching ceased and skin looked healthy on 30th day	Unpredictable (Langley et al., 2005)
6	Deep open wound in thumb toe	10-15 days	6 to 8 weeks

7	Chronic psoriasis in the neck over 10 years	Itching ceased and skin looked healthy from 30th day	Unpredictable (Langley et al., 2005)
8	Keloid on the ventral side of the hand	Pain immediately alleviated, keloid shrunken on the 60th day	Not less than 3 months. In surgical removal, mostly keloids return. (Westra et al., 2016)
9	Eczema in the dorsal aspect of the foot	16 days	Minimum of 2 weeks (Elsner et al., 2019)
10	Bleeding varicose ulcer over a dorsal foot	21 days	minimum of 12 weeks (Collins et al., 2018)
11	A punctured wound in the lateral face	5 days	2 days to 2 weeks
12	Severe psoriasis in back (Fig 4)	45 days	Unpredictable (Langley et al., 2005)
13	Vitiligo (Fig 5)	Partial to complete repigmentation by 15-25days	Minimum 3 months (Dillon et al., 2017)
14	Deep open wound in the leg	6 days	2 to 4 weeks
15	Chronic eczema in leg (Fig 6)	6 days	Minimum of 2 weeks (Elsner et al., 2019)
16	Hemorrhoids (grades 1-3)	5-16 days	Minimum a week for grade 1, a minimum of 2 weeks for grade 2, and surgery for grade 3.

Table 2: Retrospective study on coexisting diseases

No.	Systems	Diseases	Patient's feedback/ observation
1	Cardiovascular	Congestive cardiac failure with left ventricular dysfunction	The Left ventricular Ejection Fraction recorded was: On 21.02.2018: 44%; On 26.02.2018: 32%; On 05.03.2018: 18%; For back and shoulder pain, the patient started using MIRGA from 20.03.2018. But ejection fraction found to be improved on 04.04.2018 to 50%.
2	Dental	Mouth ulcer, toothache	4-6 days
3	Endocrine system	Juvenile diabetes, goiter	15-30 days
4	Integumentary system (Hair & Skin)	Allergy, alopecia areata, Hansen's disease, chronic eczema,	15-35 days
5	Musculoskeletal system	Arthritis and pain in elbow, knee and shoulder joints	The pain disappeared from 7 seconds to 5 minutes. On regular use for 15-30 days, a complete cure occurred.
6	Nervous system	Back pain, Bell's palsy, cervical spondylosis, delirium, fainting, hemiplegia, alcohol use disorder	The pain disappeared from 7 seconds to 5 minutes. Paralytic conditions cured between 30-65 days.
7	Respiratory	Respiratory system disorder	After spraying, the patent was able to inhale and exhale easier than before. Even asthmatic patients felt no discomfort during smoking.
8	Ocular	Eye SPH problem	On 28.06.2016, Left eye sphere (SPH) was 0.50. After MIRGA spraying (for 5 days to an injury near Left eyelid margin), the Left eye SPH was 0.00
9	Bites and stings	Snakebite, insect bite, wasp sting	After any bite, instant spraying alleviated pain/ burning/ irritation and prevented swelling within 2 minutes. However, for snake bites besides MIRGA spraying supportive therapy was needed.
10	Cancer*	Thyroid cancer, throat cancer, cancerous mass in the neck (4th/ metastasic stage), other malignancies	Neck cancer mass (4th stage): On the 45th day of MIRGA spraying, reduction in mass size and pain, and the patient was able to chew food much better than before. Thyroid cancer on the 15th day of spraying, the swelling reduced. Generally, after spraying pain disappearance is instantaneous, and various malignancy found to have cured between 35-240 days and no recurrence noticed. Three types of cancer cures were observed. (1) complete, (2) partial disappearance of cancer mass, (3) mass size remained the same. However, all the MIRGA treated patients showed gradual recovery from symptoms and returned to normal habits.
11	Coma		While MIRGA sprayed for traumatic wounds, concurrent recurrence of partial consciousness recorded in 15-20 days.

Table 3: Veterinary cases trialled with MIRGA (respective images available in Supplementary Table T2)

No.	Case details	MIRGA's efficacy
1	Horse –Traumatic injury	The minor and major wounds healed on 10th hour and 9th day respectively, after MIRGA spraying
2	Cow – Squamous cell carcinoma in vulval lip (Fig 7)	Before treatment: circumference 62.5cm, radius 9.96 cm. After 40 days of MIRGA spraying: circumference 50cm, radius 7.96 cm
3	Cattle –Necrosed wound in back	Healed on 10th day of MIRGA spraying
4	Dog– Senility related physical debility and disability	After MIRGA spraying for 2 months, debility improved significantly and more activity reported.
5	Dog – Recurrent idiopathic skin disorder	Completely recovered on the 12th day. Even after 6 months, no recurrence noticed.
6	Dog – Thoracic adenocarcinoma	Before treatment on 09.12.2019, the tumor mass was 5 cm; thrombocytopenia, platelet count was 79. After three months of MIRGA spraying, on 24.04.2019 size of the tumor was reduced to 2.1 cm diameter, and platelet count increased to 244.

References

1. Ganesan PC. Pendulam power of guidance & Pyramid power for success, Sura books (pvt) ltd., Chennai. 2003; p8.
2. Alberts B, Johnson A, Lewis J, Raff M, Roberts K, Walter P. The Chemical Components of a Cell. Molecular Biology of the Cell. 4th edition. New York: Garland Science. 2002.
3. Verheest F. Waves in Dusty Space Plasmas, Kluwer Academic Publishers, Netherlands. 2000; 89.
4. Sanders RH. Revealing the Heart of the Galaxy, Cambridge University Press, USA. 2014; p70
5. DeVries J. Air: The Breath of Life. Mainstream publishing company, Edinburgh. 1994.
6. Dakin JP, Brown R. Handbook of Optoelectronics: Concepts, Devices, and Techniques. Vol I, 2nd edition, CRC Press, Taylor & Francis Group, LLC. 2018; P634.
7. Aboud S, Altemimi A, Al-Hilphy A, Lee YC, Cacciola F. molecules A Comprehensive Review on Infrared Heating Applications in Food Processing. Molecules. 2019; 24: 2-21.
8. Rojas J, Gonzalez-Lima F. Low-level light therapy of the eye and brain. Eye and Brain. 2011; 3: 49-67.
9. Barolet D, Christiaens F, Hamblin M. Infrared and Skin: Friend or Foe. Journal of Photochemistry and Photobiology B: Biology. 2015; 155.
10. Chen TY, Yang YC, Sha YN, Chou JR, Liu BS. Far-Infrared Therapy Promotes Nerve Repair following End-to-End Neurorrhaphy in Rat Models of Sciatic Nerve Injury. Evidence-Based Complementary and Alternative Medicine, 2015, 1–10.
11. Perego R, Proverbio D, Zuccaro A, Spada E. Low-level laser therapy: Case-control study in dogs with sterile pyogranulomatous pododermatitis. Veterinary World. 2016; 9(8), 882–87.
12. Nagaya T, Okuyama S, Ogata F, Maruoka Y, Knapp DW, Karagiannis SN, et al., Near infrared photoimmunotherapy targeting bladder cancer with a canine anti-epidermal growth factor receptor (EGFR) antibody. Oncotarget. 2018; 9(27): 19026-19038.
13. Wardlaw JL, Gazzola KM, Wagoner A, Brinkman E, Burt J, Butler R, et al., Laser Therapy for Incision Healing in 9 Dogs. Frontiers in Veterinary Science, 2019; 5: 349.
14. Grassani D, Tagkoudi E, Guo H, Herkommer C, Yang F, Kippenberg TJ, et al., Mid infrared gas spectroscopy using efficient fiber laser driven photonic chip-based supercontinuum. Nature Communications, 2019; 10(1).
15. Toor F, Jackson S, Shang X, Arafin S, Yang H. Mid-infrared Lasers for Medical Applications: introduction to the feature issue. Biomed Opt Express. 2018; 9(12): 6255-57.
16. Musumeci F, Pollack GH. High electrical permittivity of ultrapure water at the water–platinum interface. Chemical Physics Letters. 2014; 613: 19–23.
17. Pollack GH. Cell Electrical Properties: Reconsidering the Origin of the Electrical Potential. Cell Biology International. 2015; 39(3): 237-42.
18. Sommer A, Caron A, Fecht HJ. Tuning Nanoscopic Water Layers on Hydrophobic and Hydrophilic Surfaces with Laser Light. Langmuir : the ACS journal of surfaces and colloids. 2008; 24: 635-6.
19. Sommer A, Zhu D, Mester A, Försterling HD. Pulsed Laser Light Forces Cancer Cells to Absorb Anticancer Drugs - The Role of Water in Nanomedicine. Artificial cells, blood substitutes, and immobilization biotechnology. 2011; 39(3): 169-73.
20. Mohan J. Organic Spectroscopy: Principles and Applications, 2nd edition, Alpha science international Ltd., Harrow, UK, 2004; 19.
21. Agarwal CM, Ong JL, Appleford MR, Mani G. Introduction to Biomaterials: Basic Theory with Engineering Applications. Cambridge universitypress, UK, 2014; p81.
22. Tsai SR, Hamblin MR. Biological effects and medical applications of infrared radiation, J. Photochem. Photobiol. B. 2017; 170: 197–207.
23. Flynn GW. Charles S. Parmenter, Alec M. Wodtke. Vibrational Energy Transfer. J. Phys. Chem. 1996; 100: 12817-12838.
24. Datta SN, O'Trindle C, Illas F. Theoretical and Computational Aspects of Magnetic Organic Molecules. Imperial College Press,London. 2014; p224.
25. Xu R, Xu Y. Modern Inorganic Synthetic Chemistry, 2nd edn., Elsevier B.V, Netherlands, UK, USA. 2017; 124.
26. Nouri K. Lasers in Dermatology and Medicine: Dermatologic Ap-

plications, 2nd edition, Springer International Publishing AG, Switzerland. 2018; P346.

27. Schoonover KL. Pain Free with Far Infrared Mineral Therapy. IUniverse, Inc., USA. 2003.
28. Oschman JL. Energy Medicine: The Scientific Basis, 2nd edition, Elsevier Ltd., US. 2016; p253
29. Dugdale D. Essentials of Electromagnetism, 3rd edition, American Institute of Physics, New York. 1993; p1.
30. Umakanthan, Mathi M. Decaffeination and improvement of taste, flavor and health safety of coffee and tea using mid-infrared wavelength rays. Heliyon, 2022; 8(11): e11338,
31. Umakanthan T, Mathi M. Quantitative reduction of heavy metals and caffeine in cocoa using mid-infrared spectrum irradiation. Journal of the Indian Chemical Society, 2022; 100(1).
32. Umakanthan, T, Mathi, M. Increasing saltiness of salts (NaCl) using mid-infrared radiation to reduce the health hazards. Food Science & Nutrition. 2023; 11(6): 3535– 49.
33. Umakanthan, Madhu Mathi.. Potentiation of Siddha medicine using Muppu (Universal Potentiator). International Journal of Pharmaceutical Research and Applications. 2023; 8(4): 2070-84.
34. Tishkevich DI, Korolkov IV, Kozlovskiy AL, Anisovich M, Vinnik DA, Ermekova AE, et al., Immobilization of boron-rich compound on Fe3O4 nanoparticles: Stability and cytotoxicity, J. Alloys Compd. 2019; 797: 573-81.
35. Dukenbayev K, Korolkov IV, Tishkevich DI, Kozlovskiy AL, Trukhanov SV, Gorin YG, et al., Fe3O4 nanoparticles for complex targeted delivery and boron neutron capture therapy, Nanomaterials, 2019; 494.
36. Kozlovskiy AL, Alina A, Zdorovets MV. Study of the effect of ion irradiation on increasing the photocatalytic activity of WO3 microparticles, J. Mater. Sci.: Mater. Electron. 2021; 32: 3863-77.
37. El-Shater RE, Shimy HE, Saafan SA, Darwish MA, Zhou D, Trukhanov AV, et al., Synthesis, characterization, and magnetic properties of Mn nanoferrites, J. Alloys Compd. 2022; 928: 166954.
38. Kozlovskiy AL, Zdorovets MV. Effect of doping of Ce4+/3+ on optical, strength and shielding properties of (0.5-x)TeO2-0.25MoO-0.25Bi2O3-xCeO2 glasses, Mater. Chem. Phys. 2021; 263, 124444.
39. Almessiere MA, Algarou NA, Slimani Y, Sadaqat A, Baykal A, Manikandan A, et al., 2022. Investigation of exchange coupling and microwave properties of hard/soft (SrNi0.02Zr0.01Fe11.96O19)/(CoFe2O4)x nanocomposites, Mat. Today Nano, 100186.
40. Kowacz M, Marchel M, Juknaité L, Esperança JM, Romão MJ, Carvalho AL, Rebelo LPN. Infrared light-induced protein crystallization. Structuring of protein interfacial water and periodic self-assembly. Journal of Crystal Growth, 2017; 457: 362-68.
41. McMakin C, Leon Chaitow. Frequency specific Microcurrent in pain management E-book, Elsevier, China, 2011; 30.
42. Moss D. Biomedical Applications of Synchrotron Infrared Microspectroscopy: A Practical Approach, Royal Society of Chemistry, UK, 2011; 58.
43. Yi GC. Semiconductor Nanostructures for Optoelectronic Devices: Processing, Characterization and Applications. Berlin, Heidelberg: Springer-Verlag, 2012; 198.
44. Esmaeili K. Viremedy, Homeopathic Remedies, and Energy Healing Remedies as Information – including Remedies; A Synopsis. 2015.
45. Kowacz M, Warszyński P. Effect of infrared light on protein behavior in contact with solid surfaces. Colloids and Surfaces A: Physicochemical and Engineering Aspects. 2018; 557: 94-105.
46. Volkov L, Reveguk ZV, Serdobintsev PV, Ramazanov RR, Kononov AI. DNA as UV light-harvesting antenna," Nucleic Acids Res., 2018; 46(7): 3543–51.
47. Collins L, Seraj S. Diagnosis and treatment of venous ulcers. Am Fam Physician. 2010; 81(8): 989-96.
48. American Family Physician. Taking Care of Burns. Am Fam Physician. 2000; 1;62(9): 2029-30.
49. Langley RGB, Krueger GG, Griffiths CEM. Psoriasis: epidemiology, clinical features, and quality of lifeAnnals of the Rheumatic Diseases; 2005; 64:ii 18-ii23.
50. Westra I, Pham H, Niessen FB. Topical Silicone Sheet Application in the Treatment of Hypertrophic Scars and Keloids. J Clin Aesthet Dermatol. 2016; 9(10):28-35.
51. Elsner P, Agner T. Hand eczema: treatment. Journal of the European Academy of Dermatology and Venereology, 2019; 34(S1), 13–21.
52. Dillon A B, Sideris A, Hadi A, Elbuluk N. Advances in Vitiligo: An Update on Medical and Surgical Treatments. J Clin Aesthet Dermatol. 2017; 10(1): 15-28.
53. Girard JE. Principles of Environmental Chemistry, 3rd edition, Jones & Bartlett Learning, USA. 2014; p99.
54. Shankar DR. Remote Sensing of Soils. Germany: Springer-Verlag GmbH, 2017; p268.
55. Atkins P, Paula J. Physical Chemistry for the Life Sciences, Oxford university press, Oxford, 2011; p365
56. Lee CF, Liu CY, Hsieh RH, Wei YH, 2005. Oxidative Stress-Induced Depolymerization of Microtubules and Alteration of Mitochondrial Mass in Human Cells. Annals of the New York Academy of Sciences, 2005; 1042(1): 246–54.
57. Chang HY, Shih MH, Huang HC, Tsai SR, Juan HF, Lee SC. Middle Infrared Radiation Induces G2/M Cell Cycle Arrest in A549 Lung Cancer Cells. PloS one. 2013; 8(1): e54117.
58. Chang HY, Li MH, Huang TC, Hsu CL, Tsai SR, Lee SC, et al., Quantitative Proteomics Reveals Middle Infrared Radiation-Interfered Networks in Breast Cancer Cells. Journal of Proteome Research. 2015; 14(2): 1250–62.
59. Scanlan N. Complementary Medicine for Veterinary Technicians and Nurses, Wiley-Blackwell publishing, USA. 2011.
60. Dossey L. Meaning & medicine: lessons from a doctor's tales of breakthrough and healing. Bantam publishing. 1992; P 185.
61. Fenton P, ⁋Galante L. Wisdom of tai chi: ancient secrets to health & harmony. 1998; P155.